`

Changes in chemical composition and copepod toxicity during petroleum photooxidation

Samuel D. Katz,[1,2] Haining Chen,[1,#] David M. Fields[1,3] Erin C. Beirne,[1] Phoebe Keyes,[1,#] Greg T. Drozd,[3] Christoph Aeppli[1,3,*]

(1) Bigelow Laboratory for Ocean Sciences, East Boothbay, ME, USA; *(2)* Graduate School of Oceanography, University of Rhode Island, Narragansett RI, USA; *(3)* Colby College, Waterville, ME, USA

Current Affiliation: University of Hong Kong (HC), University of Minnesota (PK)

* corresponding author caeppli@bigelow.org

TOC Figure

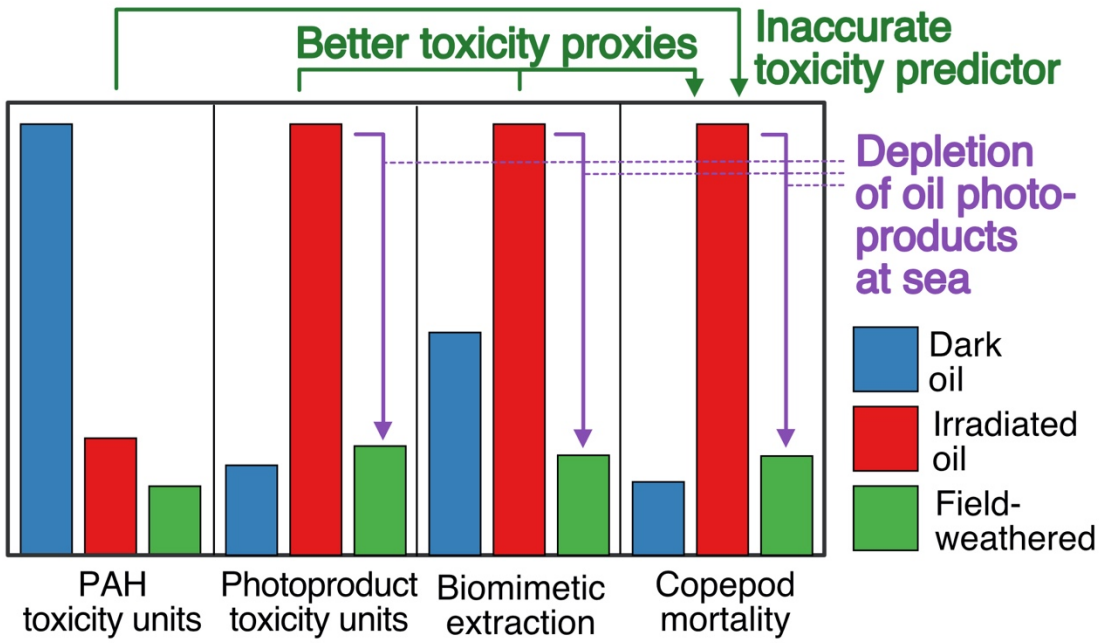

***Word count**: Abstract + Intro + Methods + Results & Discussion + 5 Figures:*
196 + 595 + 1,391 + 3,210 + 1,500 ***= 6,892 word-equivalents***

`

Abstract

Photoproducts can be formed rapidly in the initial phase of a marine oil spill. However, their toxicity is not well understood. In this study, oil was irradiated, chemically characterized, and tested for toxicity in three copepod species (*A. tonsa, T. longicornis, C.finmarchicus*). Irradiation led to a depletion of polycyclic aromatic hydrocarbons (PAHs) and *n*-alkanes in oil residues, along with an enrichment in aromatic and aliphatic oil photoproducts. Target lipid model-based calculations of PAH toxic units (TU-PAH) predicted that PAH toxicities were lower in water accommodated fractions (WAFs) of irradiated oil residues ("irradiated WAFs") than in WAFs of dark-control samples ("dark WAFs"). In contrast, biomimetic extraction (BE) measurements showed increased bioaccumulation potential of irradiated WAFs compared to dark WAFs, mainly driven by photoproducts present in irradiated oil. In line with the BE results, copepod mortality increased in response to irradiated WAFs compared to dark WAFs. Low copepod toxicities were observed for WAFs produced with photooxidized oil slicks collected during the *Deepwater Horizon* oil spill. The results of this study suggest that while oil photoproducts have the potential to be a significant source of copepod toxicity, the water solubility of these products might mitigate their toxicity at sea.

Keywords: Photoproducts, oxygenated PAHs, copepod toxicity, target lipid model, biomimetic extraction.

Synopsis: While oil irradiation leads to water-soluble photoproducts that can be toxic for copepods, their water-solubility might mitigate their environmental effect at sea.

Introduction

The transformation of hydrocarbons into oxygenated species by photooxidation of oil on the sea surface has been recognized as a major fate process of oil after the 2010 *Deepwater Horizon* (DWH) oil spill.[1–5] Of the approximately 4.1 million barrels (5.2×10^8 kg) of oil that was released into the Gulf of Mexico during this spill,[6,7] approximately 10% (5.2×10^7 kg) of that oil mass formed an oil slick or sheen at the sea surface,[8] and an estimated 54% of that was transformed from non-polar hydrocarbons into the polar fraction of oxygenated hydrocarbons (OxHC) within 5-25 days of being exposed to sunlight.[2] This OxHC fraction has been shown to enriched in oxygen and contained oxygen-containing photoproducts such as oxygenated aromatic and aliphatic compounds.[1,3,9–11] These photoproducts are currently not included in models for assessment of oil spill risk or natural resource damage, which typically only consider polycyclic aromatic hydrocarbons (PAHs), mono-aromatic compounds, and *n*-alkanes.[12,13]

While PAHs are often considered the main contributors of toxicity in crude oil,[14–16] oxygenated hydrocarbons produced by oil photooxidation are a significant contributors to toxicity in irradiated oil.[17–27] Amongst the potential photoproducts that are responsible for the observed effects, oxygenated PAHs have often been the focus due to their increased toxicity compared to their parent compounds.[22,28] Additionally, oxygenated aliphatic compounds present in tar sand processed water have also been found to be associated with ecotoxicity.[29–34]

`

Together, these studies suggest that the process of photooxidation of oil produces a complex mixture of photoproducts that influences the toxicity of the oil residue. However, there are still knowledge gaps regarding the importance of oil photoproducts to the overall oil toxicity. For example, it is often not clear to what extent irradiation-induced changes in toxicity can be explained by photoproducts vs. changes in the PAH profile caused by weathering, such as a preferential enrichment of three-ring PAHs upon evaporative losses during photooxidation.[16] Furthermore, it is difficult to assess the degree of photooxidation that led to the reported toxicity. The kinetics of oil photooxidation is dependent on many factors, including the light spectrum and intensity, the oil type, and the oil film thickness.[2,35] Lastly, while there are several proven approaches to predict toxicity of non-photooxidized oil—such as using PAH toxicity units (TU-PAH) based on the target lipid model[15,16] or biomimetic extraction methods (BE)[36,37]—it is not clear to what extent these methods can be applied to predict the toxicity of photooxidized oil.

To address these knowledge gaps and gain a better understanding of oil photo-products formation and effects, we irradiated oil, performed detailed chemical characterization of the resulting oil residues on a bulk and molecular scale, performed biomimetic extraction, predicted toxicities using target lipid model, and created water accommodated fractions (WAFs) to produce copepod toxicity assays. We chose three copepod species (*Acartia tonsa, Temora longicornis, Calanus finmarchicus*) that range from coastal to offshore animals. Copepods are the most numerically abundant multicellular zooplankton in the water column, are an important link in marine food webs [38,39] and an established model organism used to assess aquatic toxicities[40].

Note that this toxicity of oil photoproducts discussed here is different from the photo-enhanced (or photo-sensitized) toxicity that can be observed when aquatic organisms are exposed to UV light after they have accumulated PAHs.[21,41–43] Photo-enhanced toxicity is based on cell damages resulting from photochemically-produce reactive species that are formed in the organisms. In contrast, photoproducts can be formed in oil slicks that are irradiated by UV as well as visible light,[35] and can subsequently be bioaccumulated and cause toxicity in the absence of light.

Materials and Methods

Crude and Weathered Oil. DWH source oil (sample “MA”, collected from the barge *Massachusetts* on August 15, 2010) and two DWH slick oils (sample “CTC”: also referred to as “Slick A”, collected from Barge No. CTC02404 on July 29, 2010; and sample “JU”: also referred to as “Slick B”, collected from the U.S. Coast Guard Cutter *Juniper* on July 19, 2010) were obtained from BP and NOAA.[44]

Photooxidation of Crude Oil. Approx. 6 g of MA source oil was added to 90-mm glass Petri dishes (without water) to create an approx. 1 mm thick oil slick. Dishes were left open to the sunlight in a greenhouse with polycarbonate siding, which was transparent to sunlight >400 nm (Fig. S1 in the Supporting Information, SI). Dark-control samples were covered with aluminum foil and treated like the other samples. The temperature and light intensity were measured

during the experiment (Fig. S2 in the Supporting Information). At 11, 20, and 40 days, triplicates samples of irradiated and dark dishes were removed (samples Day-11, Day-20, Day-40). The oil residues were dissolved in dichloromethane (DCM), transferred to 120-mL jars, and the DCM was evaporated under a gentle stream of N_2 at 40 °C until constant weight. A second irradiation experiment was conducted with a seven-day irradiation time (samples Day-7) using MA oil that has been pre-evaporated at 98 °C for 23 h in a fume hood (resulting in 51% evaporation) before irradiation.

WAF preparation. Filtered low-energy WAFs were produced using artificial seawater and an oil loading of 1g L^{-1} following published protocols[45] with some modifications. First, water was removed from the oil residues by phase separation in a separatory funnel after dissolving the oil residues in DCM, followed by drying (Na_SSO_4) and gently evaporating the organic phase under a stream of N_2 at 40 °C until constant weight. An oil residue loading of 1g L^{-1} was used. Due to the high viscosity of some of the irradiated oil residues, all oil residues were dissolved in small volumes of DCM, added to empty 2-L glass aspirator bottles, and dried with a gentle stream of N_2 until the DCM evaporated, forming a coating of the bottom of the bottles. Artificial seawater (Sea Salt ASTM D1141-98; Lake Products Company LLC) was then added and gently stirred for 24 h with a magnetic stir bar following established protocols.[45,46] The WAFs were collected from the bottom outlet of the bottles, filtered using pre-combusted 0.47 mm GF/F filters, and used for toxicity assays. The filtration step has been shown to remove the small amounts of oil droplets that are potentially formed during low-energy WAF preparation.[47] Our modified procedure led to PAH concentrations that agreed with published values for JU WAFs (Table S5).

For chemical analysis, a volume of 500 mL of filtered WAF was spiked with *o*-terphenyl as a recovery standard (10 µL of a 4.7 mg/mL solution) and liquid/liquid extracted three times (using 15 mL, 10 mL, and 10mL of DCM). The combined organic phases were dried (Na_2SO_4) and reduced to 1 mL volume for chemical analysis.

Bulk Analytical Methods for Bulk Characterization. For bulk analysis, any traces of water were removed by dissolving the oil residues in DCM followed by evaporation of the organic phase and repeating this procedure two times. The fractions of saturated, aromatic, and oxygenated hydrocarbons (OxHC) in the extracts were quantified by thin-layer chromatography - flame ionization detection (TLC-FID) as described previously.[1] The elemental oxygen content was determined on an elemental analyzer at the UC Davis Stable Isotope Facility. The relative intensity of carbonyl functional groups ("carbonyl index") was measured on an FT-IR instrument (ThermoFisher Nicolet iS10, diamond ATR crystal, 1 cm^{-1} resolution) by normalizing carbonyl-stretching peak areas (1712 cm^{-1}) to the CH_2-peak areas (2926 cm^{-1}) following previously published methods.[1,2,48] We used peak areas rather than peak heights since this has been shown to improve accuracy.[49]

Analytical Method for Molecular Characterization. The concentrations of oil hydrocarbons and select photoproducts (Table S1) in the oil phase were performed using gas chromatography coupled to a mass spectrometer (GC/MS). The PAHs naphthalene (nap), 9H-fluorene (flu),

phenanthrene (phe), dibenzothiphene (dbt), and chrysene (chr)—along with their C_1 to C_3 alkylated congeners (nap-C1, nap-C2, nap-C3, flu-C1, etc)—and *n*-alkanes were quantified as described previously.[3] C_8 to C_{30} n-alkanoic acids were transformed into their methyl esters before analysis as described in the SI. The quantification of C_{12} to C_{30} 2-alkanones was preceded by a clean-up step with an ion-exchange resin (see Section S1). Due to chromatographic interference of (alkylated) 9H-fluorene and (alkylated) fluoren-9-one congeners, these compounds were quantified using comprehensive two-dimensional gas chromatography coupled to a time-of-flight mass spectrometer (GC×GC-TOFMS; Leco Pegasus 4D) as described in Section S1. The concentrations of oil hydrocarbons in the WAF phase were performed using solid-phase microextraction (SPME) followed by thermal desorption and GC×GC-TOF analysis, as described in the SI (Section S1).

Biomimetic Extraction (BE). A SPME coupled to a gas chromatography-flame ionization detection (GC-FID) instrument was used for BE measurements following established protocols.[37,50] Briefly, 18 mL aqueous samples were extracted in 20-mL vials for 100 min at 30 °C with a polydimethylsiloxane (PDMS) coated SPME fiber (30 µm coating, containing 0.132 µL PDMS per fiber;[51] Supelco #57289-U, Sigma-Aldrich) and an autosampler equipped with a temperature-controlled agitator (CTC CombiPAL). In order to extract acidic organic compounds, the samples were acidified to pH <3 by adding 50 µL H_3PO_4 (85%: Sigma-Aldrich). The fiber-accumulated compounds were thermally desorbed in a GC inlet in splitless mode (3 minutes at 280 °C, using a 0.75 mm Topas glass liner). The GC was equipped with a 15-m column (Rtx-1 column, 0.53 mm i.d., 1.5 µm film thickness; Restek Corp.) and an FID detector (300 °C). Helium carrier gas (17 mL min^{-1}) and the following temperature program was used: 3 min at 40°C, ramped to 300 °C at 45 °C min^{-1} (held for 10 min). After each sample, this temperature program was run for two more times without sample injection to prevent any carry-over and ensure a stable FID baseline. The total area under the FID trace was integrated, calibrated using 2,3-dimethylnaphthalene, and converted to PDMS concentrations by dividing by the volume of the SPME fiber coating according to literature.[37,50]

Copepod Toxicity Assays. *Acartia tonsa* cultures (obtained from AlgaGen LLC; Vero Beach, FL) were maintained in the lab for a minimum of two generations at 21 °C. *Calanus finmarchicus* and *Temora longicornis* were collected off-shore in the Gulf of Maine using a 300 µm and 150 µm mesh plankton net, respectively, and sorted and maintained in the laboratory at 12°C for several days before toxicity testing. All three copepod species were maintained on a 1:1 diet of *Rhodomonaus salina* (CCMP 1319) and *Thalassiosira weissflogii* (CCMP 1051), obtained from the National Center of Marine Algae and Microbiota (NCMA, Bigelow Laboratory, East Boothbay, ME).

A. tonsa copepod toxicity was tested by incubating 20 adult females in 100 mL WAF (or dilution thereof) in a glass jar for 24 h at room temperature. Each test was conducted in triplicates, and controls were prepared using artificial seawater instead of WAFs. *T. longicornis* toxicity assays were conducted at 12 °C but with otherwise identical conditions as *A. tonsa*. *C. finmarchicus* toxicity assays were performed according to literature,[52] by incubating 14

copepods per L of seawater for 96 hours. The mortality was determined by counting moving and non-moving copepods. Analysis of variance (Holm-Sidak method) was performed in SigmaPlot (Systat Software Inc., San Jose, CA), and dose-response curve fitting was performed using the drc R package (log-logistic function LL2.2).[53]

Toxicity Unit Calculations. Baseline toxicity effect concentrations ($LC_{50,i}$) of compounds i were estimated based on the target lipid model,[14,54] using a critical lipid concentration (C_{crit}) and liposome-water partition coefficients ($K_{lip\text{-}w,i}$) of compound i:

$$LC_{50,i} = \frac{C_{crit}}{K_{lip-w,i}} \quad \text{(eq.1)}$$

A C_{crit} of 100 mmol (kg lipids)$^{-1}$ was used, which is a conservative estimate applicable for many species of algae, fish and invertebrates.[55–57] $K_{lip\text{-}w}$ of hydrocarbons and photoproducts were calculated using the COSMO-RS method as implemented in the COSMOtherm and COSMOmic program suite (COSMOlogic GmbH), as described in the SI (Section S2.2 and Table S8). Toxicity Unit (TU) values were calculated as the sum of TU_i of all compounds *i*:

$$\mathrm{TU} = \sum_i TU_i = \sum_i \frac{C_{i,aq}}{LC_{50,i}} \quad \text{(eq.2)}$$

Thereby, the aqueous concentration of compound *i* ($C_{i,aq}$) was estimated from its concentration in the oil phase using Raoult's law (following approaches described in literature[58]) and COSMOtherm-calculated seawater solubilities (see Section S2 for details).

Results and Discussion

Changes in Bulk Oil Properties During Irradiation. The bulk oxygen content, carbonyl index, and the polar oil fraction ("OxHC fraction") of oil residues is an indicator of oil photooxidation.[1–3] We observed increases in these metrics in the oil irradiated in our experimental system (Figure 1A). Oxygen content increased up to 500% in the Day-40 sample (relative to the original MA oil), carbonyl index increased by 560%, and the relative amount of the OxHC fraction increased by 160% (Table S2). In the dark controls the increase in these properties was consistent with evaporation, but was less pronounced than that in the irradiated samples. The field-collected slick samples the CTC oil reached similar degrees of oxygenation as our most oxygenated samples based on these bulk properties (irradiated Day-40 sample), while the JU oil exceeded this degree of oxygenation.

While our experimental system was able to approximate photooxidation processes that occur at sea, it differed in four aspects. First, our experimental irradiance (average of 1.84 kW m^{-2} d^{-1}) was approx. 3.6 times lower than that observed on the Gulf of Mexico sea surface during the DWH oil spill (6.44 kW m^{-2} d^{-1}; Fig S2). Our 40-day irradiation would, therefore, correspond to 11 days on the Gulf of Mexico sea surface. Second, we used a film thickness of approx 1mm, while the estimated average oil film thickness during the *Deepwater Horizon* was

`

219 70 μm,[59] although the film thickness was likely heterogeneous and variable over time at sea.
220 The greater thickness of oil films diminishes light penetration[2] and decreases oxygen diffusion[60]
221 which reduces the rate of photooxidation. We, therefore, expect that our irradiated oil would
222 photooxidize slower than at sea during the *Deepwater Horizon* oil spill. Third, our experimental
223 irradiation was conducted in a greenhouse without contribution from UV light <400nm (Fig. S1).
224 We previously established that the majority (>80%) of oil photo-oxidation by sunlight is caused
225 by visible light (>400nm),[2] in line with other studies that found oil photooxidation using light in
226 the visible range,[60,61] or at reduced UV irradiation (at 5 m depth in seawater or under 50 cm of
227 sea ice).[62,63] Fourth, we conducted the photooxidation experiments in the absence of water, in
228 line with previous laboratory experiments.[64] Since the source of oxygen incorporated into the oil
229 is mainly molecular O_2 rather than H_2O,[35] the photooxidation mechanism is not expected to be
230 influenced by the absence of water. Furthermore, our oil residue will not lose any photoproducts
231 due to dissolution until WAFs are prepared. Overall, while our oil exposure differs from an oil
232 sheen at the sea surface, we still expect that the process of oil photooxidation in our system are
233 comparable to that at sea.
234
235 **Molecular Changes During Irradiation:** On a molecular level, samples had a lower
236 concentration of PAHs and *n*-alkanes after irradiation (Fig. 1C-D). This enhanced loss in the
237 irradiated samples was mainly related to loss of two-ring PAHs and lower-molecular-weight *n*-
238 alkanes, and resulted from the combined effects of photooxidation and evaporation. The
239 irradiated samples experienced a higher evaporative loss than the dark-control samples (31 to
240 35% and 36-45% evaporation based on gravimetry, respectively; Table S9), since the black oil
241 exposed to the sunlight led to a higher sample temperature when irradiated compared to the
242 aluminum foil-covered dark-control samples.
243 The relative depletion of compounds compared to the original MA oil showed that *n*-
244 alkanes followed an evaporation behavior, with lower-molecular compounds being more
245 depleted than higher-molecular weight compounds in dark as well as in irradiated samples (Fig.
246 S3). In contrast, a deviation from that behavior was observed for four-ring PAHs in irradiated
247 samples, with chrysene and its alkylated congeners being more depleted than expected based
248 on evaporation alone (Fig. S3). This depletion is in line with photochemical transformation of
249 PAHs and also agrees with changes in bulk properties (oxygen, carbonyl index, OxHC fraction)
250 in the irradiated samples described above.
251 Along with degradation of *n*-alkanes and PAHs, we observed increasing concentrations
252 of *n*-alkanoic acids, 2-alkanones, as well as fluoren-9-one and its alkylated congeners (C_0 to C_3-
253 oxFlu) with irradiation for all samples (Fig. 1B). While oxygenated oxFlu congeners can be
254 formed photochemically from fluorene precursors,[18] *n*-alkanoic acids and 2-alkenones form
255 through photosensitized *n*-alkane photooxidation.[65,66]
256 Overall, the depletion pattern for PAHs and *n*-alkanes suggests that PAHs are more
257 photochemically reactive than *n*-alkanes. Such a behavior has been observed previously,[67,68]
258 and is in line with a direct[69] or indirect photooxidation mechanisms of PAHs,[60,70,71] along with the
259 radial-mediated degradation of saturated compounds[65,72,73] as a minor side reaction. The

appearance of aliphatic and aromatic photoproducts is evidence that both reactions are co-occurring.

The field slick samples CTC and JU showed a similar evaporative depletion pattern of PAHs and *n*-alkanes, along with a photodegradation depletion signal in PAHs, as our irradiated samples (Fig 1C-D, Fig. S3). Interestingly, the photoproduct pattern of sample JU looked somewhat different than our oxygenated samples: while comparable amounts of aliphatic photoproducts were present, significantly less oxFlu was present in JU than in irradiated Day-40 sample. It is likely that these relatively water-soluble photoproducts were depleted though dissolution in the field slick samples.

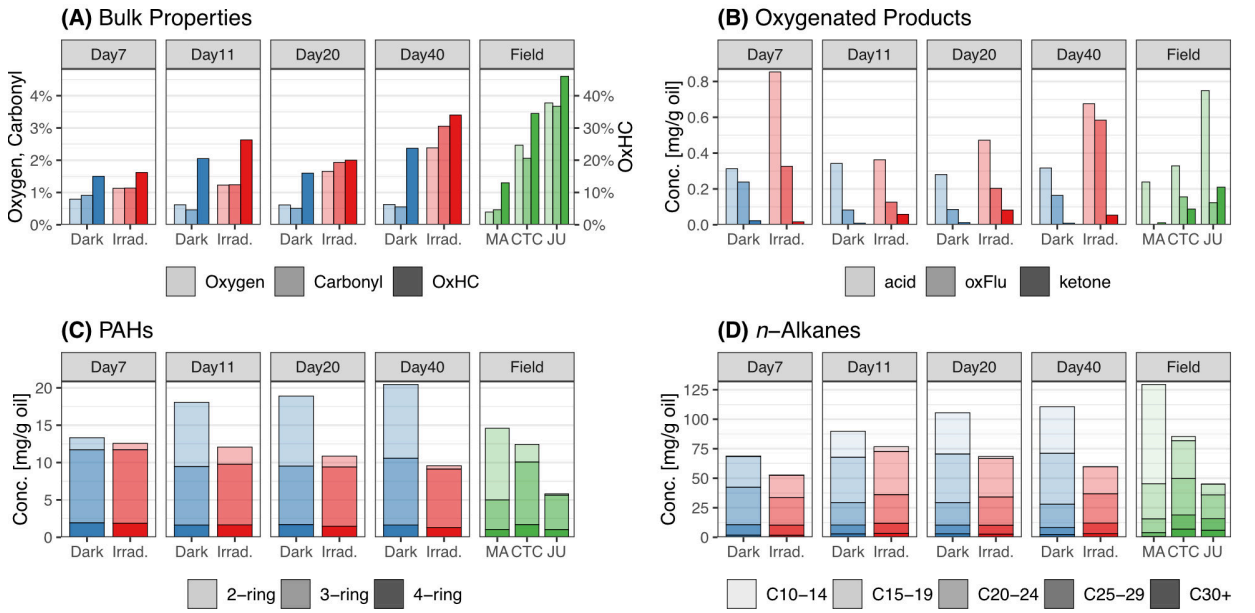

Figure 1: *Chemical characterization dark-control (blue bars), irradiated (red bars) and and field-collected DWH oil samples (green bars). (A) bulk properties showing the oxygen content (oxygen), FT-IR determined carbonyl index (carbonyl), and TLC-FID determined OxHC fraction (OxHC, right y-axis). (B) Concentration of quantified photoproduct in oil residues, including n-alkanoic acids (acids), 2-alkenones (ketones), and C_0 to C_3 fluorene-9-one congeners (oxFlu). (C) PAH and concentrations in oil residues. Given are the sums of parent and alkylated congeners of 2-ring PAHs (naphthalene congeners), 3-ring PAHs (fluorene, phenanthrene, and dibenzothiophene congeners), and 4-ring PAHs (chrysene congeners). (D) Concentrations of groups of n-alkanes. Given are the carbon number groupings indicated in the legend.*

Change in WAF Chemistry Upon Oil Irradiation. PAH concentration profiles of the WAFs produced with the irradiated samples ("irradiated WAFs") and with the dark-control samples ("dark WAFs") were in agreement with the corresponding oil concentrations. For example, since dark and irradiated Day-7 oils (which were pre-evaporated) had similar PAH concentration profiles (Fig. 1C), their WAF concentrations were also similar (17 and 21 µg L^{-1} for the irradiated and dark WAF, respectively; Fig 2A). The slightly lower PAH concentration in the irradiated oil

samples and corresponding WAFs are consistent with the observed photooxidation and increased evaporation of these oil samples (Fig 1C).

In contrast, WAFs prepared with the irradiated (but not pre-evaporated) Day-40 oils, had a much lower total PAH concentration than the dark WAFs (17 μg L^{-1} and 132 μg L^{-1}, respectively; Fig 2B). This difference was driven by alkylated two-ring PAHs, which were evaporated or photooxidized in the irradiated Day-40 oil samples (Fig. 1C). WAFs prepared with the field-collected slick JU oil had the lowest total PAH concentration of approx. 2 μg L^{-1}, in agreement with literature values in the range of 4±2 μg L^{-1}.[45] In addition to photooxidation and evaporation, the low concentration in JU oil can be attributed to loss of PAHs due to dissolution of these relatively water-soluble PAHs during its ascent through the water column and its 7-9 days residence time on the sea surface prior to collection.[64]

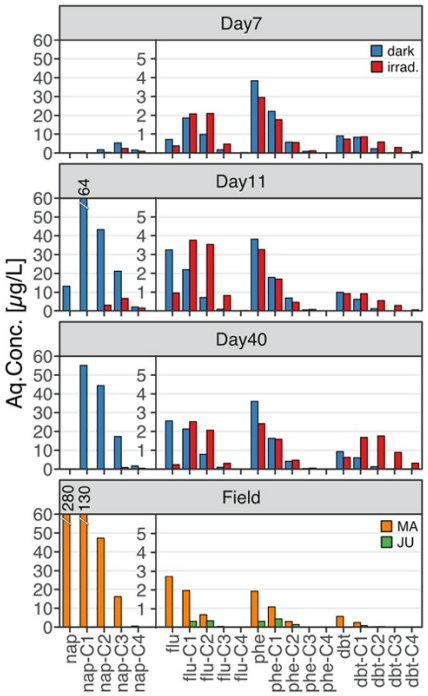

Figure 2. *Measured concentrations of PAHs in water accommodated fractions (WAFs) prepared with dark-control (blue bars) and irradiated (red bars) oil exposed for 7, 11, and 40 days and with the DWH source oil (MA; orange bars) and field-weathered JU oil (orange bar). Naphthalene and three-ring PAH concentrations are given on different scales.*

To further analyze the WAF concentrations, we predicted aqueous concentrations based on the chemical composition of the oil residues and Raoult's law (Fig. 3B). Thereby, we used calculated PAH water solubilities and estimated average molecular weights of oil residues (Section S2.3 and Table S9). The resulting concentrations agreed with measured concentrations within an order of magnitude for 97% of the measurements (Fig. 3A). The measured values were lower than the predicted ones by an average factor of 3.9±3.6 (n=100), likely due to non-equilibrium conditions in the 18-h WAFs, evaporation of volatile compounds

during WAF generation, or by overpredicted water solubility or average molecular weights of the oil residues by the computational method. Still, the predicted PAH distribution profile agreed with measured profiles, with two-ring PAH concentrations mainly driving the differences between irradiated and dark WAFs (Fig 3B). Note that the lower measured vs. predicted concentrations suggest that no oil droplets were present in our WAFs (or were removed during the filtration process), as this would have resulted in increased measured values of *n*-alkanes and water-insoluble heavy PAHs.

Predicted PAHs Toxicities. We used a target lipid model[14,54] to estimate the PAH toxicity of WAFs produced with the investigated oil residues (Fig. 3C). The lipid-accumulated mass was calculated from WAF concentrations and lipid-water partition coefficients, and related to a critical lipid concentration that would result in 50% lethality (LC_{50}) or other effect in the organisms. The toxicity of a WAF is expressed as toxicity unit (TU), with a TU = 1 representing a summed aqueous concentration of all bioaccumulating compounds that lead to the critical lipid concentration (see Methods Section and Section S2.3). Since individual oil hydrocarbons have varying lipid-accumulation properties, the use of TU is superior in predicting toxicities than the use of the total dissolved PAH concentration (tPAH).[74,75]

Our calculated TU values predict that dark WAFs have higher toxicities than irradiated WAFs for all time points (Fig. 3C). The difference in toxicity between dark and irradiated WAFs of any time point was mainly driven by two-ring PAHs, while the contribution of three-ring PAHs was comparable in irradiated and dark WAFs. Due to their low aqueous solubilities, the four-ring PAHs played an insignificant role in the calculated PAH-TUs. For field-collected oil residues, WAF produced with the more oxygenated JU oil (JU-WAF) had lower TU values than the CTC-WAF. Overall, the calculation predicts that the PAH-associated toxicity decreases with photooxidation of oil samples. This would be in line with decreasing toxicities as oil weathers through evaporation, as has been shown before.[16,76]

Caution has to be applied when interpreting the time series of dark-control WAFs. Note that evaluating toxicity associated with weathering processes can be complicated by employing our approach of using constant oil loading to prepare WAFs, without correcting the oil mass for evaporative oil losses. As previous studies have shown, using a fixed loading of a series of evaporated oils leads to an apparent increase in toxicity with increasing evaporation due to the preferential enrichment of the bioaccumulative PAHs with evaporation of lighter compounds.[77,78] Since we did not correct for evaporative losses, an apparent increasing PAH toxicity can be seen in our dark WAFs along the time series of Day-11 to Day-40 (Fig 3C). However, given that our dark and irradiated oil residues had comparable degrees of evaporative loss at each time point (Table S9), comparing dark to irradiated WAFs at any time point is still valid despite constant oil loadings in all WAFs.

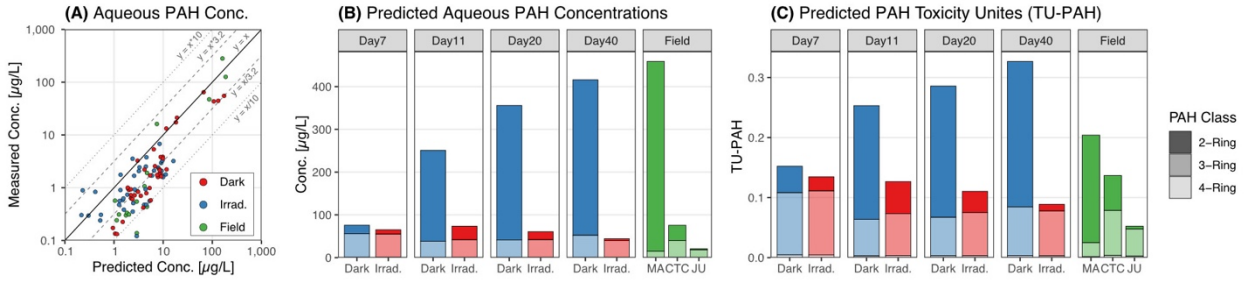

Figure 3. *(A) Comparison of predicted and measured PAH concentrations in WAFs. (B) Predicted aqueous PAHs concentrations based on measured oil concentrations. Two-, three-, and four-ring PAHs are given in different shades. (C) Corresponding calculated contributions of PAHs to toxicity (expressed as PAH toxicity units, TU-PAH), based on the chemical composition of oil residues and a target lipid model.*

Biomimetic Extraction Reveals Bioaccumulative Photoproducts: An alternative to the theoretical TU calculation is the experimental determination of compounds that can accumulate in hydrophobic phases (such as lipids). This can be accomplished using the BE method, which is based on equilibration of compounds between an aqueous phase and a thin hydrophobic phase (30 µm PDMS) bound to a fiber by using solid-phase microextraction (SPME).[79,80] Biomimetic extraction methods have been successfully used to assess the toxicity of WAFs that contain hydrocarbons as well as carboxyl-containing petroleum-derived products for a range aquatic species.[37,81]

We performed biomimetic extraction measurements using WAFs produced with Day-7, Day-11, Day-40, and JU oil (Fig. 4). In contrast to the TU-PAH predictions, we found that the irradiated WAFs led to an equal or greater mass of compounds accumulated on the fiber for all investigated time points than the dark WAFs (Fig. 4A-C). These biomimetic extraction results, along with measured PAH concentrations, implies that bioavailable non-PAH compounds are present in irradiated WAFs. The GC-FID chromatograms from Day-40 show that the non-PAH bioaccumulative compounds are mainly part of an unresolved complex mixture (UCM)-like hump in the chromatogram (Fig. 4C). This hump disappears when the biomimetic extraction is performed at pH-neutral rather than acidic conditions (pH < 2; Fig. 4C, black FID trace). Such a pH-depended sorption of compounds has previously been observed in oil sand process water (OSPW) with carboxyl-containing petroleum-derived products.[81] While these organic acids sorb into polymer-coated fibers only in their neutral form,[82] but are still bioaccumulative in their ionized form due to the charged nature of biological membranes.[83] Our BE results suggest the presence of organic acids in irradiated WAFs. The increased carbonyl index (Fig. 1A) and *n*-alkanoic acid content in our irradiated oil residues (Fig. 1D) would support the presence of such compounds.

Interestingly, the JU WAF did not appear to contain significant amounts of bioaccumulative organic acids (Fig. 4D). As discussed above, the water solubility of these compounds likely led to their depletion during the estimated 8 to 9 days this slick spent on the sea surface.[2]

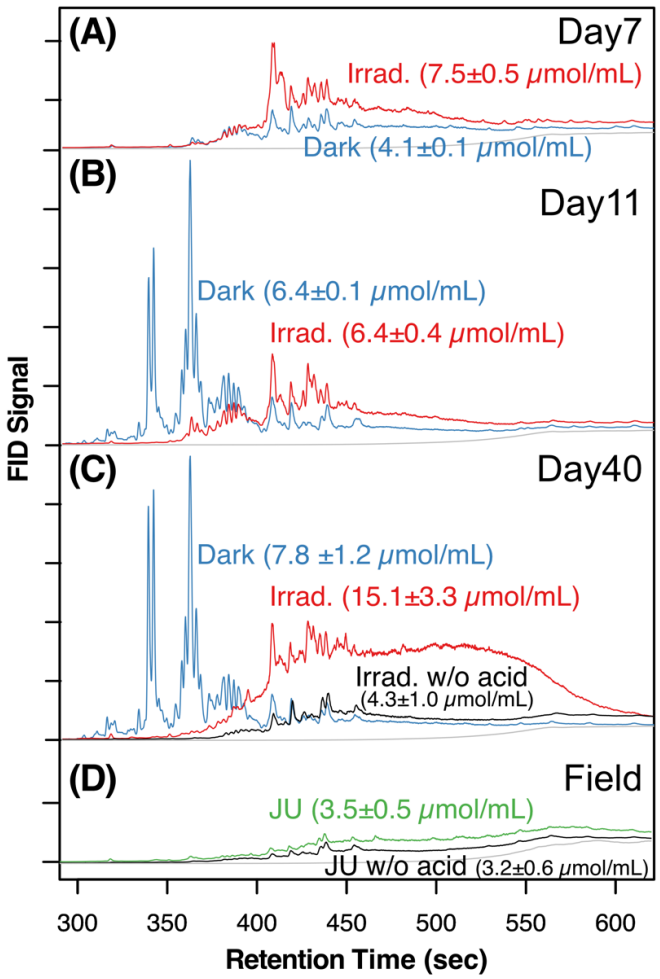

Figure 4*: Biomimetic extraction (BE) results. Shown are SPME-GC-FID chromatograms of WAFs prepared with dark-control (blue lines) and irradiated (red lines) oil residues collected at (A) timepoint D7, (B) timepoint D11, (C) timepoint D40, and (D) with Juniper oil (JU green line). Given is the total mass of compounds sorbed to the SPME fiber, representative of bioaccumulative compounds. For the D7 and D40 timepoint, more compounds accumulated in the irradiated WAF than in the dark-control WAFs. This additional accumulation disappeared in the D40 timepoint when the irradiated WAF was extracted at neutral pH (w/o acid; black line). This is consistent with carboxylic acid-containing photoproduct being bioaccumulative products. WAFs prepared with JU seem to contain little such photoproducts.*

Enhanced Copepod Mortality of WAFs Produced with Irradiated Oil. We tested the acute copepod toxicity of dark and irradiated WAFs. First, we acquired dose-response curves using dilution series of WAFs produced with the Day-7 oil samples (Fig. 5A). The irradiated and dark oils of this time point, as well as the resulting WAFs, had similar PAH profiles and concentrations as the irradiated oil (Fig 1C, Fig 2A, Tables S3 and S4). Despite the similar PAH concentrations, we found significantly higher toxicity of irradiated WAF than dark WAF for all three tested copepod species (*A. tonsa, T. longicornis, and C. finmarchicus*; Fig. 5A). Fitted

`

404 ln(LC_{50}) values were significantly different between the two treatments for both *A. tonsa* and *T.*
405 *longicornis*, and the dark and irradiated 100% WAF treatments were significantly different in the
406 *C. finmarchicus* experiment ($p < 0.05$; Tables S6-S7). We conclude that oil irradiation led to the
407 molecular changes that resulted in a significant enhancement of copepod toxicity across
408 different species. Based on the TU-PAH calculation, this toxicity enhancement was not caused
409 by PAHs (Fig 3A).
410 To assess the impact of degree of photooxidation on copepod toxicity, we then tested
411 the *A. tonsa* toxicity using undiluted (i.e., 100%) WAFs produced with the time series of
412 irradiated and dark oil residues Day-11, Day-20, and Day-40 (Fig. 5B). In line with the results
413 using the Day-7 WAFs, all WAFs produced with irradiated oil exhibited significantly higher
414 mortality than the WAFs produced with dark-control oil ($p < 0.05$; Fig. 2B, Table S6). This higher
415 mortality was despite lower total PAH concentrations (Fig. 2, Table S5) and lower predicted TU-
416 PAH (Fig. 3C, Table S10) in all irradiated WAFs than in the dark WAFs. Again, the PAH
417 concentration was not the driver of copepod toxicity in the irradiated samples.
418 WAFs produced with the field-collected CTC and JU oil slicks led to low toxicities (Fig.
419 4B), even though these oil residues had a similar or higher degree of photooxidation than our
420 irradiated Day-40 oil sample, based on bulk properties (Fig. 1A). This finding of low mortality of
421 these slick oils are constant with published results.[84]
422

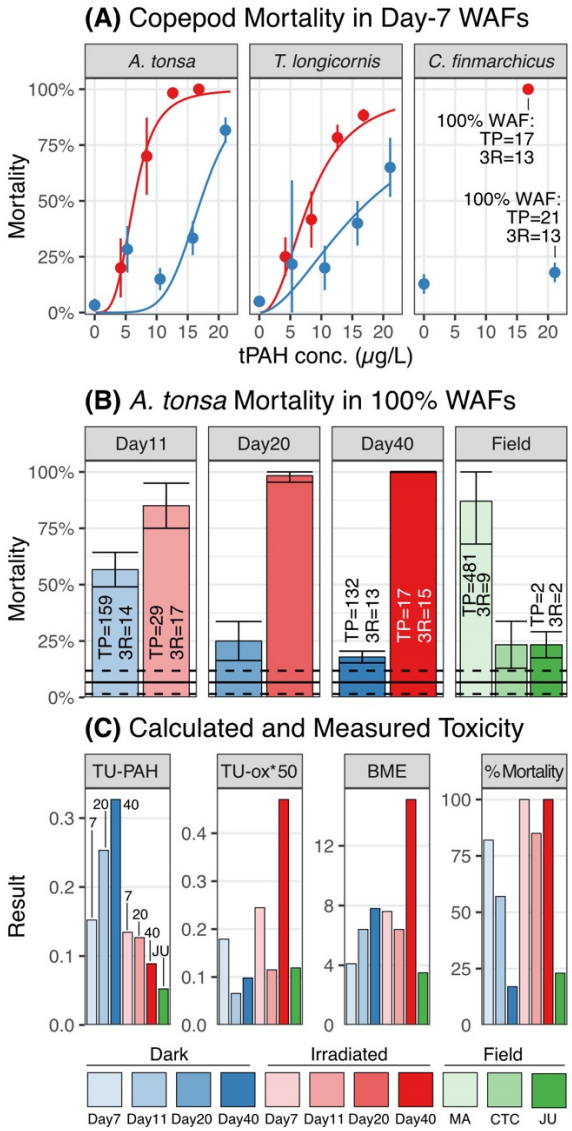

Figure 5*: Measured and calculated toxicities of WAFs produced with irradiated, dark-control, and field-collected oil residues. (A) Dose-response results of dilution series of WAFs produced with the 7-day irradiated (red) and dark-controls (blue) oils using three copepod species. Lines are fitted using a log-logistic dose-response function. Measured total PAHs (TP) and three-ring PAH (3R) concentration for 100%-WAFs are given in the last panel (in µg L^{-1}) (B) A. tonsa lethality of 100%-WAFs produced with oil exposed for 11, 20, and 40 days. The measured total PAHs and three-ring PAH concentration (TP and 3R; in µg L^{-1}) and the average (±1σ) seawater blank from six replicates (horizontal lines) are given. (C) Overview of calculated toxicity unites for PAHs (TU-PAH), toxicity units for oxygenated compounds (TU-ox; scaled by a factor of 50), measured biomimetic extraction (BE) fiber accumulation (in µmol/mL), and A. tonsa lethality of 100% WAFs (%Mortality) produced with dark and irradiated oils exposed for 11, 20, and 20 days and the field-weathered JU oil. TU-ox and BE are better proxies for toxicities than TU-PAH.*

`

Contribution of Photoproducts to Copepod Toxicity. Given that PAHs are not the primary toxins in our laboratory-generated samples, we examined the potential contribution of oil photoproducts for observed copepod toxicity. In contrast to TU-PAH values, trends in the biomimetic extraction were in a general agreement with the toxicity results (Fig. 5C). For example, the irradiated WAFs produced higher fiber accumulation than the dark WAFs for the Day-7 and the Day-40 time point, in agreement with the observed toxicity results. We also calculated TUs based on the quantified oxygenated photoproducts ("TU-ox"). Thereby, LC_{50} values were estimated based on predicted lipid-water partition coefficients in the same way as we calculated TU-PAH values for PAHs (see Section S2 for details). Resulting TU-ox values suggest that for each time point, the irradiated WAFs have a higher toxicity contribution from photoproducts than for dark WAFs, in line with observed copepod toxicities (Fig. 5C). Amongst the analyzed compounds, oxFlu had a greater contribution to TU-ox than 2-alkanones or *n*-alkanoic acids Table S10). This observation might point to the greater relative contribution of PAH photoproducts than aliphatic photoproducts to the overall toxicity of photooxidized oil.

The calculated TU-ox values were roughly 50 times lower than calculated TU-PAH. The small TU-ox values is partially a result of the quantified photoproducts being only a small fraction of the total amount of oxygenated oil compounds present in the samples,[3] whereas a more comprehensive characterization of PAHs and *n*-alkanes was possible. For example, the total concentration of quantified oil photoproducts was 1.3 mg g^{-1} for the Day-40 irradiated sample, which was <1% of its OxHC fraction (Fig. 1 and Tables S2 and S4). Therefore, the calculated TU-ox would not reflect of the toxicity of all photoproducts. As is evident from the broad and unresolved peaks in the biomimetic extraction results (Fig. 4), photoproducts are a complex mixture of compounds that are inherently difficult to quantify on a molecular level. Due to their polarity and thermal lability, many photoproducts are outside the analytical window of the employed analytical techniques (GC/MS, in combination with chemical modification).[85] A larger spectrum of oil photoproducts was identified in irradiated oil using liquid chromatography[86] or direct infusion followed by high-resolution MS.[9,11,87] However, these methods are not yet able to quantify these products. Our calculated TU-ox values are, therefore, a proxy for toxicity rather than a representation of the entire photo-product toxicity. For a more accurate determination of TU-ox, quantitative methods to measure a larger fraction of the photoproducts will have to be developed.

In contrast to experimentally irradiated oil, WAFs produced using DWH slick oil residues showed relatively low copepod mortality (Fig. 2B), even though DHW slick samples have a high degree of oil photooxidation (Fig 1A). The difference in toxicity between our laboratory-irradiated and the field-collected oil samples likely originates from the depletion of water-soluble compounds that occurred when the slick samples were on the sea surface for 5 to 25 days.[2] The oxygenation of hydrocarbons decreases their hydrophobicity as measured by the octanol-water partition coefficient by 1-2 orders of magnitude,[3] likely leading to a depletion of these products after formation. Our irradiated samples were generated in the absence of water, preserving soluble photoproducts in the oil phase until the generation of the WAFs. These soluble compounds contributed to a large fraction of the bioaccumulative compounds, as can be seen from comparing the biomimetic extraction results of Day-40 and JU (Fig. 4). Furthermore,

biodegradation of oil hydrocarbons or photoproducts might have occurred on the sea surface. Although octadecane/pristane ratios in DWH slick samples did not point to extensive oil biodegradation,[2] increased microbial oxygen consumption under DWH oil slicks suggests active microbial oil hydrocarbon degradation at sea.[88]

Implications for the Toxicity of Photooxidized Oil. The enhanced toxicity of irradiated oil has implications for the assessment of the risk and damage of marine oil spills and for further research on the fate and effect of oil photoproducts. First, the observed toxicity of oil photoproducts on copepods raises questions about toxicity towards other aquatic organisms. While Increased fish toxicity of the more photooxidized JU relative to the CTC oil residue has been attributed to preferential enrichment of three-ring PAHs,[89–93] oil photoproducts might also play a role in fish toxicity.[27] More research to quantify the toxicity contribution of oil photoproduct to various aquatic organisms is necessary.

Second, since polar and ionized compounds have been shown to contribute to baseline toxicity in a similar way as PAHs,[56,94] photoproducts should be included when using a TU approach to predict toxicity of weathered oil based on its composition. In order to accurately predict the toxicity of photooxidized oil from its chemical composition, quantitative analytical methods and reference materials need to be developed to quantify a larger proportion of oil photoproducts. Alternatively, approaches like the biomimetic extraction method may provide a suitable tool for estimating the toxicity of photooxidized oil towards aquatic organisms.

Third, the reduced toxicities of DWH field samples (JU and CTC) compared to our laboratory-irradiated samples suggests that the dissolution and potentially biodegradation of oil photoproducts can mitigate the toxicity of the oil slicks on the sea surface. However, the extent and time scale in which dissolution and biodegradation determines the environmental fate of oil photoproducts still need to be constrained better in future research.

Acknowledgments

Nina Forziati, Anna Van Dreser, and Tom Regan are acknowledged for producing preliminary data for this study, and Hannah Karp is acknowledged for performing FT-IR measurements. This research was made possible by grants from the Gulf Research Program (2000008903) and NSF (OCE 1460861).

Associated Content

Supporting Information. The Supporting Information is available free of charge on the ACS Publications website.

- Document with additional methods details (Section S1), and approach for calculating properties and TU values of compounds (Section S2); Supporting Tables including names and abbreviations of analyzed compounds (Table S1), bulk measurements results (Table S2), PAH and *n*-alkane concentrations in oil residues (Table S3), OxHC concentrations in oil residues

`

(Table S4), PAH concentrations in WAFs (Table S5), copepod toxicity results (Table S6), LC50 statistics (Table S7), calculated physico-chemical properties and LC50 values (Table S8), Estimated average oil molecular weight values (Table S9), calculated TUs for investigated oil residues (Table S10), results from biomimetic extraction analysis (Table S11): Supporting Figures including solar spectrum during irradiation (Fig. S1), temperature and light intensity during irradiation (Fig. S2), and remaining fractions of *n*-alkanes and PAHs in investigated samples (Fig. S3) (PDF).

- Spreadsheets of Table S1 to S11 (XLSX).

References

(1) Aeppli, C.; Carmichael, C. A.; Nelson, R. K.; Lemkau, K. L.; Graham, W. M.; Redmond, M. C.; Valentine, D. L.; Reddy, C. M. Oil Weathering after the Deepwater Horizon Disaster Led to the Formation of Oxygenated Residues. *Environ. Sci. Technol.* **2012**, *46* (16), 8799–8807.

(2) Ward, C. P.; Sharpless, C. M.; Valentine, D. L.; French McCay, D. P.; Aeppli, C.; White, H. K.; Rodgers, R. P.; Gosselin, K. M.; Nelson, R. K.; Reddy, C. M. Partial Photochemical Oxidation Was a Dominant Fate of Deepwater Horizon Surface Oil. *Environ. Sci. Technol.* **2018**, *52* (4), 1797–1805.

(3) Aeppli, C.; Swarthout, R. F.; O'Neil, G. W.; Katz, S. D.; Nabi, D.; Ward, C. P.; Nelson, R. K.; Sharpless, C. M.; Reddy, C. M. How Persistent and Bioavailable Are Oxygenated Deepwater Horizon Oil Transformation Products? *Environ. Sci. Technol.* **2018**, *52* (13), 7250–7258.

(4) Ward, C. P.; Overton, E. B. How the 2010 Deepwater Horizon Spill Reshaped Our Understanding of Crude Oil Photochemical Weathering at Sea: A Past, Present, and Future Perspective. *Environ. Sci. Process. Impacts* **2020**, *22* (5), 1125–1138.

(5) Aeppli, C. Recent Advance in Understanding Photooxidation of Hydrocarbons after Oil Spills. *Curr. Opin. Chem. Eng.* **2022**, *36* (100763), 100763.

(6) McNutt, M.; Camilli, R.; Guthrie, G.; Hsieh, P.; Labson, V. *Assessment of Flow Rate Estimates for the Deepwater Horizon/Macondo Well Oil Spill. Flow Rate Technical Group Report to the National Incident Command*; 2011.

(7) McNutt, M. K.; Camilli, R.; Crone, T. J.; Guthrie, G. D.; Hsieh, P. A.; Ryerson, T. B.; Savas, O.; Shaffer, F. Review of Flow Rate Estimates of the Deepwater Horizon Oil Spill. *Proc. Natl. Acad. Sci. U. S. A.* **2012**, *109* (50), 20260–20267.

(8) Ryerson, T. B.; Camilli, R.; Kessler, J. D.; Kujawinski, E. B.; Reddy, C. M.; Valentine, D. L.; Atlas, E.; Blake, D. R.; de Gouw, J.; Meinardi, S.; Parrish, D. D.; Peischl, J.; Seewald, J. S.; Warneke, C. Chemical Data Quantify Deepwater Horizon Hydrocarbon Flow Rate and Environmental Distribution. *Proc. Natl. Acad. Sci. U. S. A.* **2012**, *109* (50), 20246–20253.

(9) Ruddy, B. M.; Huettel, M.; Kostka, J. E.; Lobodin, V. V.; Bythell, B. J.; McKenna, A. M.; Aeppli, C.; Reddy, C. M.; Nelson, R. K.; Marshall, A. G.; Rodgers, R. P. Targeted Petroleomics: Analytical Investigation of Macondo Well Oil Oxidation Products from Pensacola Beach. *Energy Fuels* **2014**, *28* (6), 4043–4050.

(10) Cao, X.; Tarr, M. A. Aldehyde and Ketone Photoproducts from Solar-Irradiated Crude Oil-Seawater Systems Determined by Electrospray Ionization-Tandem Mass Spectrometry. *Environ. Sci. Technol.* **2017**, *51* (20), 11858–11866.

(11) Huba, A. K.; Gardinali, P. R. Characterization of a Crude Oil Weathering Series by Ultrahigh-Resolution Mass Spectrometry Using Multiple Ionization Modes. *Sci. Total Environ.* **2016**, *563–564*, 600–610.

(12) Spaulding, M. L. State of the Art Review and Future Directions in Oil Spill Modeling. *Mar. Pollut. Bull.* **2017**, *115* (1–2), 7–19.
(13) French McCay, D. P. Oil Spill Impact Modeling: Development and Validation. *Environ. Toxicol. Chem.* **2004**, *23* (10), 2441–2456.
(14) Di Toro, D. M.; McGrath, J. A.; Hansen, D. J. Technical Basis for Narcotic Chemicals and Polycyclic Aromatic Hydrocarbon Criteria. I. Water and Tissue. *Environ. Toxicol. Chem.* **2000**, *19* (8), 1951–1970.
(15) Di Toro, D. M.; McGrath, J. A. Technical Basis for Narcotic Chemicals and Polycyclic Aromatic Hydrocarbon Criteria. II. Mixtures and Sediments. *Environ. Toxicol. Chem.* **2000**, *19* (8), 1971–1982.
(16) Di Toro, D. M.; McGrath, J. A.; Stubblefield, W. A. Predicting the Toxicity of Neat and Weathered Crude Oil: Toxic Potential and the Toxicity of Saturated Mixtures. *Environ. Toxicol. Chem.* **2007**, *26* (1), 24–36.
(17) Hansen, H. P. Photochemical Degradation of Petroleum Hydrocarbon Surface Films on Seawater. *Mar. Chem.* **1975**, *3* (3), 183–195.
(18) Larson, R. A.; Hunt, L. L.; Blankenship, D. W. Formation of Toxic Products from a #2 Fuel Oil by Photooxidation. *Environ. Sci. Technol.* **1977**, *11* (5), 492–496.
(19) Larson, R. A.; Bott, T. L.; Hunt, L. L.; Rogenmuser, K. Photooxidation Products of a Fuel Oil and Their Antimicrobial Activity. *Environ. Sci. Technol.* **1979**, *13* (8), 965–969.
(20) Pengerud, B.; Thingstad, F.; Tjessem, K.; Aaberg, A. Photo-Induced Toxicity of North Sea Crude Oils toward Bacterial Activity. *Mar. Pollut. Bull.* **1984**, *15* (4), 142–146.
(21) Huang, X.-D.; Krylov, S. N.; Ren, L.; McConkey, B. J.; Dixon, D. G.; Greenberg, B. M. Mechanistic Quantitative Structure-Activity Relationship Model for the Photoinduced Toxicity of Polycyclic Aromatic Hydrocarbons: II. An Empirical Model for the Toxicity of 16 Polycyclic Aromatic Hydrocarbons to the Duckweed Lemna Gibba L. G-3. *Environ. Toxicol. Chem.* **1997**, *16* (11), 2296–2303.
(22) McConkey, B. J.; Duxbury, C. L.; Dixon, D. G.; Greenberg, B. M. Toxicity of a PAH Photooxidation Product to the Bacteria Photobacterium Phosphoreum and the Duckweed Lemna Gibba: Effects of Phenanthrene and Its Primary Photoproduct, Phenanthrenequinone. *Environ. Toxicol. Chem.* **1997**, *16* (5), 892–899.
(23) Maki, H.; Sasaki, T.; Harayama, S. Photo-Oxidation of Biodegraded Crude Oil and Toxicity of the Photo-Oxidized Products. *Chemosphere* **2001**, *44* (5), 1145–1151.
(24) Shemer, H.; Linden, K. G. Aqueous Photodegradation and Toxicity of the Polycyclic Aromatic Hydrocarbons Fluorene, Dibenzofuran, and Dibenzothiophene. *Water Research*. 2007, pp 853–861. https://doi.org/10.1016/j.watres.2006.11.022.
(25) Rial, D.; Radović, J. R.; Bayona, J. M.; Macrae, K.; Thomas, K. V.; Beiras, R. Effects of Simulated Weathering on the Toxicity of Selected Crude Oils and Their Components to Sea Urchin Embryos. *J. Hazard. Mater.* **2013**, *260*, 67–73.
(26) Zito, P.; Podgorski, D. C.; Johnson, J.; Chen, H.; Rodgers, R. P.; Guillemette, F.; Kellerman, A. M.; Spencer, R. G. M.; Tarr, M. A. Molecular-Level Composition and Acute Toxicity of Photosolubilized Petrogenic Carbon. *Environ. Sci. Technol.* **2019**, *53* (14), 8235–8243.
(27) Kim, D.; Jung, J.-H.; Ha, S. Y.; An, J. G.; Shankar, R.; Kwon, J.-H.; Yim, U. H.; Kim, S. H. Molecular Level Determination of Water Accommodated Fraction with Embryonic Developmental Toxicity Generated by Photooxidation of Spilled Oil. *Chemosphere* **2019**, *237*, 124346.
(28) Mallakin, A.; McConkey, B. J.; Miao, G.; McKibben, B.; Snieckus, V.; Dixon, D. G.; Greenberg, B. M. Impacts of Structural Photomodification on the Toxicity of Environmental Contaminants: Anthracene Photooxidation Products. *Ecotoxicol. Environ. Saf.* **1999**, *43* (2), 204–212.
(29) Clemente, J. S.; Fedorak, P. M. A Review of the Occurrence, Analyses, Toxicity, and

Biodegradation of Naphthenic Acids. *Chemosphere* **2005**, *60* (5), 585–600.
(30) Frank, R. A.; Kavanagh, R.; Kent Burnison, B.; Arsenault, G.; Headley, J. V.; Peru, K. M.; Van Der Kraak, G.; Solomon, K. R. Toxicity Assessment of Collected Fractions from an Extracted Naphthenic Acid Mixture. *Chemosphere* **2008**, *72* (9), 1309–1314.
(31) Frank, R. A.; Fischer, K.; Kavanagh, R.; Kent Burnison, B.; Arsenault, G.; Headley, J. V.; Peru, K. M.; Van Der Kraak, G.; Solomon, K. R. Effect of Carboxylic Acid Content on the Acute Toxicity of Oil Sands Naphthenic Acids. *Environmental Science & Technology*. 2009, pp 266–271. https://doi.org/10.1021/es8021057.
(32) Jones, D.; Scarlett, A. G.; West, C. E.; Rowland, S. J. Toxicity of Individual Naphthenic Acids to Vibrio Fischeri. *Environ. Sci. Technol.* **2011**, *45* (22), 9776–9782.
(33) Bartlett, A. J.; Frank, R. A.; Gillis, P. L.; Parrott, J. L.; Marentette, J. R.; Brown, L. R.; Hooey, T.; Vanderveen, R.; McInnis, R.; Brunswick, P.; Shang, D.; Headley, J. V.; Peru, K. M.; Hewitt, L. M. Toxicity of Naphthenic Acids to Invertebrates: Extracts from Oil Sands Process-Affected Water versus Commercial Mixtures. *Environ. Pollut.* **2017**, *227*, 271–279.
(34) Dogra, Y.; Scarlett, A. G.; Rowe, D.; Galloway, T. S.; Rowland, S. J. Predicted and Measured Acute Toxicity and Developmental Abnormalities in Zebrafish Embryos Produced by Exposure to Individual Aromatic Acids. *Chemosphere* **2018**, *205*, 98–107.
(35) Ward, C. P.; Sharpless, C. M.; Valentine, D. L.; Aeppli, C.; Sutherland, K. M.; Wankel, S. D.; Reddy, C. M. Oxygen Isotopes (δ 18 O) Trace Photochemical Hydrocarbon Oxidation at the Sea Surface. *Geophys. Res. Lett.* **2019**, *46*, 6745 –6754.
(36) Redman, A. D.; Parkerton, T. F.; Letinski, D. J.; Manning, R. G.; Adams, J. E.; Hodson, P. V. Evaluating Toxicity of Heavy Fuel Oil Fractions Using Complementary Modeling and Biomimetic Extraction Methods. *Environ. Toxicol. Chem.* **2014**, *33* (9), 2094–2104.
(37) Redman, A. D.; Butler, J. D.; Letinski, D. J.; Di Toro, D. M.; Leon Paumen, M.; Parkerton, T. F. Technical Basis for Using Passive Sampling as a Biomimetic Extraction Procedure to Assess Bioavailability and Predict Toxicity of Petroleum Substances. *Chemosphere* **2018**, *199*, 585–594.
(38) Runge, J. A. Should We Expect a Relationship between Primary Production and Fisheries? The Role of Copepod Dynamics as a Filter of Trophic Variability. In *Biology of Copepods*; Springer Netherlands, 1988; pp 61–71.
(39) Schminke, H. K. Entomology for the Copepodologist. *J. Plankton Res.* **2007**, *29* (suppl_1), i149–i162.
(40) Lopes, L. F. de P.; Agostini, V. O.; Moreira, R. A.; Muxagata, E. Acartia Tonsa Dana 1849 as a Model Organism: Considerations on Acclimation in Ecotoxicological Assays. *Bull. Environ. Contam. Toxicol.* **2021**, *106* (5), 734–739.
(41) Duesterloh, S.; Short, J. W.; Barron, M. G. Photoenhanced Toxicity of Weathered Alaska North Slope Crude Oil to the Calanoid Copepods Calanus Marshallaeand Metridia Okhotensis. *Environ. Sci. Technol.* **2002**, *36* (18), 3953–3959.
(42) Incardona, J. P.; Vines, C. A.; Linbo, T. L.; Myers, M. S.; Sloan, C. A.; Anulacion, B. F.; Boyd, D.; Collier, T. K.; Morgan, S.; Cherr, G. N.; Scholz, N. L. Potent Phototoxicity of Marine Bunker Oil to Translucent Herring Embryos after Prolonged Weathering. *PLoS One* **2012**, *7* (2), e30116.
(43) Marzooghi, S.; Finch, B. E.; Stubblefield, W. A.; Di Toro, D. M. Predicting Phototoxicity of Alkylated PAHs, Mixtures of PAHs, and Water Accommodated Fractions (WAF) of Neat and Weathered Petroleum with the Phototoxic Target Lipid Model. *Environ. Toxicol. Chem.* **2018**, *37* (8), 2165–2174.
(44) BP Gulf Science Data. Chemical analysis and physical properties of weathered, unweathered, and surrogate crude oils from the Deepwater Horizon accident in the Gulf of Mexico, July 2010 to January 2011 https://data.gulfresearchinitiative.org/data/BP.x750.000:0003 (accessed 2019 -10 -12). https://doi.org/10.7266/N7R78CM9.

(45) Forth, H. P.; Mitchelmore, C. L.; Morris, J. M.; Lipton, J. Characterization of Oil and Water Accommodated Fractions Used to Conduct Aquatic Toxicity Testing in Support of the Deepwater Horizon Oil Spill Natural Resource Damage Assessment. *Environ. Toxicol. Chem.* **2017**, *36* (6), 1450–1459.
(46) Singer, M. M.; Aurand, D.; Bragin, G. E.; Clark, J. R. Standardization of the Preparation and Quantitation of Water-Accommodated Fractions of Petroleum for Toxicity Testing. *Marine pollution …* **2000**. https://doi.org/10.1016/S0025-326X(00)00045-X.
(47) Forth, H. P.; Mitchelmore, C. L.; Morris, J. M.; Lay, C. R.; Lipton, J. Characterization of Dissolved and Particulate Phases of Water Accommodated Fractions Used to Conduct Aquatic Toxicity Testing in Support of the Deepwater Horizon Natural Resource Damage Assessment. *Environ. Toxicol. Chem.* **2017**, *36* (6), 1460–1472.
(48) White, H. K.; Wang, C. H.; Williams, P. L.; Findley, D. M.; Thurston, A. M.; Simister, R. L.; Aeppli, C.; Nelson, R. K.; Reddy, C. M. Long-Term Weathering and Continued Oxidation of Oil Residues from the Deepwater Horizon Spill. *Mar. Pollut. Bull.* **2016**, *113* (1–2), 380–386.
(49) Almond, J.; Sugumaar, P.; Wenzel, M. N.; Hill, G.; Wallis, C. Determination of the Carbonyl Index of Polyethylene and Polypropylene Using Specified Area under Band Methodology with ATR-FTIR Spectroscopy. *E-polymers* **2020**, *20* (1), 369–381.
(50) Letinski, D.; Parkerton, T.; Redman, A.; Manning, R.; Bragin, G.; Febbo, E.; Palandro, D.; Nedwed, T. Use of Passive Samplers for Improving Oil Toxicity and Spill Effects Assessment. *Mar. Pollut. Bull.* **2014**, *86* (1–2), 274–282.
(51) Bruno, T. J.; Svoronos, P. D. N. *CRC Handbook of Basic Tables for Chemical Analysis*, 0 ed.; CRC Press, 2010.
(52) Hansen, B. H.; Altin, D.; Rørvik, S. F.; Øverjordet, I. B.; Olsen, A. J.; Nordtug, T. Comparative Study on Acute Effects of Water Accommodated Fractions of an Artificially Weathered Crude Oil on Calanus Finmarchicus and Calanus Glacialis (Crustacea: Copepoda). *Sci. Total Environ.* **2011**, *409* (4), 704–709.
(53) Ritz, C.; Baty, F.; Streibig, J. C.; Gerhard, D. Dose-Response Analysis Using R. *PLoS One* **2015**, *10* (12), e0146021.
(54) Redman, A. D.; Parkerton, T. F.; Leon Paumen, M.; Butler, J. D.; Letinski, D. J.; den Haan, K. A Re-Evaluation of PETROTOX for Predicting Acute and Chronic Toxicity of Petroleum Substances. *Environ. Toxicol. Chem.* **2017**, *36* (8), 2245–2252.
(55) McGrath, J. A.; Parkerton, T. F.; Di Toro, D. M. Application of the Narcosis Target Lipid Model to Algal Toxicity and Deriving Predicted-No-Effect Concentrations. *Environ. Toxicol. Chem.* **2004**, *23* (10), 2503–2517.
(56) Escher, B. I.; Baumer, A.; Bittermann, K.; Henneberger, L.; K nig, M.; K hnert, C.; Kluver, N. General Baseline Toxicity QSAR for Nonpolar, Polar and Ionisable Chemicals and Their Mixtures in the Bioluminescence Inhibition Assay with Aliivibrio Fischeri. *Environ. Sci. Process. Impacts* **2017**, *19* (3), 414–428.
(57) McGrath, J. A.; Fanelli, C. J.; Di Toro, D. M.; Parkerton, T. F.; Redman, A. D.; Paumen, M. L.; Comber, M.; Eadsforth, C. V.; den Haan, K. Re-Evaluation of Target Lipid Model-Derived HC5 Predictions for Hydrocarbons. *Environ. Toxicol. Chem.* **2018**, *19*, 1951.
(58) Kang, H.-J.; Lee, S.-Y.; Roh, J.-Y.; Yim, U. H.; Shim, W. J.; Kwon, J.-H. Prediction of Ecotoxicity of Heavy Crude Oil: Contribution of Measured Components. *Environ. Sci. Technol.* **2014**, *48* (5), 2962–2970.
(59) MacDonald, I. R.; Garcia-Pineda, O.; Beet, A.; Daneshgar Asl, S.; Feng, L.; Graettinger, G.; French-McCay, D.; Holmes, J.; Hu, C.; Huffer, F.; Leifer, I.; Muller-Karger, F.; Solow, A.; Silva, M.; Swayze, G. Natural and Unnatural Oil Slicks in the Gulf of Mexico. *J. Geophys. Res. C: Oceans* **2015**, *120* (12), 8364–8380.
(60) Lichtenthaler, R. G.; Haag, W. R.; Mill, T. Photooxidation of Probe Compounds Sensitized by Crude Oils in Toulene and as an Oil Film on Water. *Environ. Sci. Technol.*

1989, *23* (1), 39–45.
(61) Corrêa, R. J.; Severino, D.; Souza, R. da S.; de Santana, E. F.; Mauro, L. L.; Alvarenga, S. D. S.; Nicodem, D. E. The Generation of Singlet Oxygen by Petroleum and Its Fractions. *J. Photochem. Photobiol. A Chem.* **2012**, *236*, 9–13.
(62) Vergeynst, L.; Greer, C. W.; Mosbech, A.; Gustavson, K.; Meire, L.; Poulsen, K. G.; Christensen, J. H. Biodegradation, Photooxidation and Dissolution of Petroleum Compounds in an Arctic Fjord during Summer. *Environ. Sci. Technol.* **2019**.
(63) Vergeynst, L.; Christensen, J. H.; Kjeldsen, K. U.; Meire, L.; Boone, W.; Malmquist, L. M. V.; Rysgaard, S. In Situ Biodegradation, Photooxidation and Dissolution of Petroleum Compounds in Arctic Seawater and Sea Ice. *Water Res.* **2019**, *148*, 459–468.
(64) Ward, C. P.; Armstrong, C. J.; Conmy, R. N.; French-McCay, D. P.; Reddy, C. M. Photochemical Oxidation of Oil Reduced the Effectiveness of Aerial Dispersants Applied in Response to the Deepwater Horizon Spill. *Environ. Sci. Technol. Lett.* **2018**, *5* (5), 226–231.
(65) Rontani, J.-F.; Giral, P. J.-P. Significance of Photosensitized Oxidation of Alkanes During the Photochemical Degradation of Petroleum Hydrocarbon Fractions in Seawater. *Int. J. Environ. Anal. Chem.* **1990**, *42* (1–4), 61–68.
(66) Rontani, J.-F. Identification by GC/MS of Acidic Compounds Produced During the Photosensitized Oxidation of Normal and Isoprenoid Alkanes in Seawater. *Int. J. Environ. Anal. Chem.* **1991**, *45* (1), 1–9.
(67) Garrett, R. M.; Pickering, I. J.; Haith, C. E.; Prince, R. C. Photooxidation of Crude Oils. *Environ. Sci. Technol.* **1998**, *32* (23), 3719–3723.
(68) King, S. M.; Leaf, P. A.; Olson, A. C.; Ray, P. Z.; Tarr, M. A. Photolytic and Photocatalytic Degradation of Surface Oil from the Deepwater Horizon Spill. *Chemosphere* **2014**, *95*, 415–422.
(69) Fasnacht, M. P.; Blough, N. V. Mechanisms of the Aqueous Photodegradation of Polycyclic Aromatic Hydrocarbons. *Environ. Sci. Technol.* **2003**, *37* (24), 5767–5772.
(70) Larson, R. A.; Hunt, L. L. Photooxidation of a Refined Petroleum Oil: Inhibition by β-Carotene and Role of Singlet Oxygen. *Photochem. Photobiol.* **1978**, *28* (4–5), 553–555.
(71) Plata, D. L.; Sharpless, C. M.; Reddy, C. M. Photochemical Degradation of Polycyclic Aromatic Hydrocarbons in Oil Films. *Environ. Sci. Technol.* **2008**, *42* (7), 2432–2438.
(72) Gesser, H. D.; Wildman, T. A.; Tewari, Y. B. Photooxidation of N-Hexadecane Sensitized by Xanthone. *Environ. Sci. Technol.* **1977**, *11* (6), 605–608.
(73) Guiliano, M.; El Anba-Lurot, F.; Doumenq, P.; Mille, G.; Rontani, J. F. Photo-Oxidation of n-Alkanes in Simulated Marine Environmental Conditions. *J Photoch Photobio A* **1997**, *102* (2–3), 127–132.
(74) Redman, A. D.; Parkerton, T. F. Guidance for Improving Comparability and Relevance of Oil Toxicity Tests. *Mar. Pollut. Bull.* **2015**, *98* (1–2), 156–170.
(75) National Academies of Sciences, Engineering; Medicine. *The Use of Dispersants in Marine Oil Spill Response*; The National Academies Press: Washington, DC, 2019.
(76) Maloney, E. M.; Naile, J.; Saunders, D. M. V. Quantifying the Effect of Weathering on Acute Oil Toxicity Using the PETROTOX Model. *Mar. Pollut. Bull.* **2021**, *162*, 111849.
(77) Carls, M. G.; Rice, S. D.; Hose, J. E. Sensitivity of Fish Embryos to Weathered Crude Oil: Part I. Low-Level Exposure during Incubation Causes Malformations, Genetic Damage, and Mortality in Larval Pacific Herring (Clupea Pallasi). *Environ. Toxicol. Chem.* **1999**, *18* (3), 481–493.
(78) Bellas, J.; Saco-Álvarez, L.; Nieto, Ó.; Bayona, J. M.; Albaiges, J.; Beiras, R. Evaluation of Artificially-Weathered Standard Fuel Oil Toxicity by Marine Invertebrate Embryogenesis Bioassays. *Chemosphere* **2013**, *90* (3), 1103–1108.
(79) Mayer, P.; Vaes, W. H.; Hermens, J. L. Absorption of Hydrophobic Compounds into the Poly(Dimethylsiloxane) Coating of Solid-Phase Microextraction Fibers: High Partition

Coefficients and Fluorescence Microscopy Images. *Anal. Chem.* **2000**, *72* (3), 459–464.
(80) Parkerton, T. F.; Stone, M. A.; Letinski, D. J. Assessing the Aquatic Toxicity of Complex Hydrocarbon Mixtures Using Solid Phase Microextraction. *Toxicol. Lett.* **2000**, *112–113*, 273–282.
(81) Redman, A. D.; Parkerton, T. F.; Butler, J. D.; Letinski, D. J.; Frank, R. A.; Hewitt, L. M.; Bartlett, A. J.; Gillis, P. L.; Marentette, J. R.; Parrott, J. L.; Hughes, S. A.; Guest, R.; Bekele, A.; Zhang, K.; Morandi, G.; Wiseman, S.; Giesy, J. P. Application of the Target Lipid Model and Passive Samplers to Characterize the Toxicity of Bioavailable Organics in Oil Sands Process-Affected Water. *Environ. Sci. Technol.* **2018**, *52* (14), 8039–8049.
(82) Escher, B. I.; Berg, M.; Mühlemann, J.; Schwarz, M. A. A.; Hermens, J. L. M.; Vaes, W. H. J.; Schwarzenbach, R. P. Determination of Liposome/Water Partition Coefficients of Organic Acids and Bases by Solid-Phase Microextraction. *Analyst* **2002**, *127* (1), 42–48.
(83) Bittermann, K.; Spycher, S.; Endo, S.; Pohler, L.; Huniar, U.; Goss, K.-U.; Klamt, A. Prediction of Phospholipid-Water Partition Coefficients of Ionic Organic Chemicals Using the Mechanistic Model COSMOmic. *J. Phys. Chem. B* **2014**, *118* (51), 14833–14842.
(84) Faksness, L. G.; Altin, D.; Nordtug, T.; Daling, P. S.; Hansen, B. H. Chemical Comparison and Acute Toxicity of Water Accommodated Fraction (WAF) of Source and Field Collected Macondo Oils from the Deepwater Horizon Spill. *Mar. Pollut. Bull.* **2015**, *91* (1), 222–229.
(85) McKenna, A. M.; Rodgers, R. P.; Nelson, R. K.; Reddy, C. M.; Savory, J. J.; Kaiser, N. K.; Fitzsimmons, J. E.; Marshall, A. G. Expansion of the Analytical Window for Oil Spill Characterization by Ultrahigh Resolution Mass Spectrometry: Beyond Gas Chromatography. *Environ. Sci. Technol.* **2013**, 130521150737003.
(86) Payne, J. R.; Phillips, C. R. Photochemistry of Petroleum in Water. *Environ. Sci. Technol.* **1985**, *19* (7), 569–579.
(87) Niles, S. F.; Chacón-Patiño, M. L.; Chen, H.; McKenna, A. M.; Blakney, G. T.; Rodgers, R. P.; Marshall, A. G. Molecular-Level Characterization of Oil-Soluble Ketone/Aldehyde Photo-Oxidation Products by Fourier Transform Ion Cyclotron Resonance Mass Spectrometry Reveals Similarity Between Microcosm and Field Samples. *Environmental Science & Technology*. 2019, pp 6887–6894. https://doi.org/10.1021/acs.est.9b00908.
(88) Edwards, B. R.; Reddy, C. M.; Camilli, R.; Carmichael, C. A.; Longnecker, K.; Van Mooy, B. A. S. Rapid Microbial Respiration of Oil from the Deepwater Horizon Spill in Offshore Surface Waters of the Gulf of Mexico. *Environ. Res. Lett.* **2011**, *6* (3). https://doi.org/10.1088/1748-9326/6/3/035301.
(89) Brette, F.; Machado, B.; Cros, C.; Incardona, J. P.; Scholz, N. L.; Block, B. A. Crude Oil Impairs Cardiac Excitation-Contraction Coupling in Fish. *Science* **2014**, *343* (6172), 772–776.
(90) Incardona, J. P.; Gardner, L. D.; Linbo, T. L.; Brown, T. L.; Esbaugh, A. J.; Mager, E. M.; Stieglitz, J. D.; French, B. L.; Labenia, J. S.; Laetz, C. A.; Tagal, M.; Sloan, C. A.; Elizur, A.; Benetti, D. D.; Grosell, M.; Block, B. A.; Scholz, N. L. Deepwater Horizon Crude Oil Impacts the Developing Hearts of Large Predatory Pelagic Fish; 2014; Vol. 111, pp E1510–E1518.
(91) Esbaugh, A. J.; Mager, E. M.; Stieglitz, J. D.; Hoenig, R.; Brown, T. L.; French, B. L.; Linbo, T. L.; Lay, C.; Forth, H.; Scholz, N. L.; Incardona, J. P.; Morris, J. M.; Benetti, D. D.; Grosell, M. The Effects of Weathering and Chemical Dispersion on Deepwater Horizon Crude Oil Toxicity to Mahi-Mahi (Coryphaena Hippurus) Early Life Stages. *Sci. Total Environ.* **2016**, *543* (Pt A), 644–651.
(92) Echols, B.; Smith, A.; Gardinali, P. R.; Rand, G. M. Chronic Toxicity of Unweathered and Weathered Macondo Oils to Mysid Shrimp (Americamysis Bahia) and Inland Silversides (Menidia Beryllina). *Arch. Environ. Contam. Toxicol.* **2016**, *71* (1), 78–86.
(93) O'Shaughnessy, K. A.; Forth, H.; Takeshita, R.; Chesney, E. J. Toxicity of Weathered Deepwater Horizon Oil to Bay Anchovy (Anchoa Mitchilli) Embryos. *Ecotoxicol. Environ.*

Saf. **2018**, *148*, 473–479.
(94) Meador, J. P.; Nahrgang, J. Characterizing Crude Oil Toxicity to Early-Life Stage Fish Based On a Complex Mixture: Are We Making Unsupported Assumptions? *Environ. Sci. Technol.* **2019**, *53* (19), 11080–11092.